PROCEEDINGS B

royalsocietypublishing.org/journal/rspb

Research

Cite this article: Chisholm RA *et al*. 2024 Assessing the spatial scale of synchrony in forest tree population dynamics. *Proc. R. Soc. B* **291**: 20240486.
https://doi.org/10.1098/rspb.2024.0486

Received: 27 February 2024
Accepted: 15 October 2024

Subject Category:
Ecology

Subject Areas:
ecology

Keywords:
population dynamics, synchrony, forest trees, Moran effect

Author for correspondence:
Ryan A. Chisholm
e-mail: ryan.chis@gmail.com

Electronic supplementary material is available online at https://doi.org/10.6084/m9.figshare.c.7508869.

Assessing the spatial scale of synchrony in forest tree population dynamics

Ryan A. Chisholm[1], Tak Fung[1], Kristina J. Anderson-Teixeira[2,3], Norman A. Bourg[2], Warren Y. Brockelman[5,6], Sarayudh Bunyavejchewin[7,8], Chia-Hao Chang-Yang[10], Yu-Yun Chen[11], George B. Chuyong[12], Richard Condit[13], Handanakere S. Dattaraja[14], Stuart J. Davies[3], Sisira Ediriweera[15], Corneille E. N. Ewango[16], Edwino S. Fernando[18,19], I. A. U. Nimal Gunatilleke[20], C. V. Savitri Gunatilleke[20], Zhanqing Hao[21], Robert W. Howe[23], David Kenfack[24], Tze Leong Yao[25], Jean-Remy Makana[17], Sean M. McMahon[26,4], Xiangcheng Mi[27,28], Mohizah Bt. Mohamad[29], Jonathan A. Myers[30], Anuttara Nathalang[5], Álvaro J. Pérez[31], Sangsan Phumsathan[8,9], Nantachai Pongpattananurak[7,8], Haibao Ren[27,28], Lillian J. V. Rodriguez[32], Raman Sukumar[14], I-Fang Sun[11], Hebbalalu S. Suresh[14], Duncan W. Thomas[33], Jill Thompson[34], Maria Uriarte[35], Renato Valencia[31], Xugao Wang[22], Amy T. Wolf[23] and Jess K. Zimmerman[36]

[1]Department of Biological Sciences, Faculty of Science, National University of Singapore, 14 Science Drive 4, Singapore 117558, Singapore
[2]Conservation Ecology Center, Smithsonian's National Zoo & Conservation Biology Institute, Front Royal, VA 22630, USA
[3]Forest Global Earth Observatory, and [4]Forest Global Earth Observatory, Smithsonian Tropical Research Institute, Washington, DC 20013, USA
[5]National Biobank of Thailand, National Science and Technology Development Agency, Science Park, Paholyothin Road, Khlong Luang, Pathum Thani 12120, Thailand
[6]Institute of Molecular Biosciences, Mahidol University, Salaya, Phutthamonthon 4 Road, Nakhon Pathom 73170, Thailand
[7]Department of Forest Biology, [8]Thai Long-term Forest Ecological Research Project, Faculty of Forestry, and [9]Department of Conservation, Faculty of Forestry, Kasetsart University, Bangkok 10900, Thailand
[10]Department of Biological Sciences, National Sun Yat-sen University, Kaohsiung 80424
[11]Department of Natural Resources and Environmental Studies, National Dong Hwa University, Hualien 97401
[12]Department of Plant Science, University of Buea, Buea PO Box 63, Cameroon
[13]Retired
[14]Centre for Ecological Sciences, Indian Institute of Science, Bangalore 560012, India
[15]Department of Science and Technology, Faculty of Applied Sciences, Uva Wellassa University, Badulla 90000, Sri Lanka
[16]Faculty of Sustainable Management of Renewable Resources, and [17]Faculty of Sciences, University of Kisangani, Kisangani R408, Democratic Republic of Congo
[18]Department of Forest Biological Sciences, The University of the Philippines - Los Baños, Laguna 4031, Philippines
[19]Institute of Biology, University of the Philippines Diliman, Quezon City, 1101, Philippines
[20]Department of Botany, University of Peradeniya, Peradeniya 20400, Sri Lanka
[21]State Key Laboratory of Forest and Soil Ecology, and [22]State Key Laboratory of Forest Ecology and Silvicuture, Institute of Applied Ecology, Chinese Academy of Sciences, Shenyang, Liaoning 110164
[23]Department of Natural and Applied Sciences, University of Wisconsin-Green Bay, Green Bay, WI 54311, USA
[24]Department of Botany, MRC-166, Smithsonian Institution, PO Box 37012, Washington, DC 20013-7012, USA
[25]Forestry and Environment Division, Forest Research Institute Malaysia, Kepong, Selangor 52109, Malaysia
[26]Smithsonian Environmental Research Center, 647 Contees Wharf Road, Edgewater, MD 21037-0028, USA
[27]Zhejiang Qianjiangyuan Forest Biodiversity National Observation and Research Station, State Key Laboratory of Vegetation and Environmental Change, Institute of Botany, Chinese Academy of Sciences, Beijing 100093
[28]National Botanical Garden, Beijing 100093
[29]International Affairs Division, Forest Department Sarawak, Tkt 13, Bangunan Baitulmakmur 2, Medan Raya, Petra Jaya, Kuching, Sarawak 93050, Malaysia
[30]Department of Biology, Washington University in St Louis, St Louis, MO 63130, USA
[31]Escuela de Ciencias Biológicas, Pontificia Universidad Católica del Ecuador, Apartado, Quito 17-01-2184, Ecuador

THE ROYAL SOCIETY PUBLISHING

[32]Institute of Biology, University of the Philippines Diliman, Quezon City 1101, Philippines
[33]Department of Botany and Plant Pathology, Oregon State University, Corvallis, OR 97331, USA
[34]UK Centre for Ecology & Hydrology, Bush Estate, Penicuik, Midlothian EH26 0QB, UK
[35]Department of Ecology, Evolution & Environmental Biology, Columbia University, New York, NY 10027, USA
[36]Department of Environmental Sciences, University of Puerto Rico, San Juan, PR 00925, USA

RAC, 0000-0002-9847-1710; TF, 0000-0003-1039-4157; RC, 0000-0003-4191-1495; SJD, 0000-0002-8596-7522; SMM, 0000-0001-8302-6908; XM, 0000-0002-2971-5881; I-FS, 0000-0001-9749-8324

Populations of forest trees exhibit large temporal fluctuations, but little is known about the synchrony of these fluctuations across space, including their sign, magnitude, causes and characteristic scales. These have important implications for metapopulation persistence and theoretical community ecology. Using data from permanent forest plots spanning local, regional and global spatial scales, we measured spatial synchrony in tree population growth rates over sub-decadal and decadal timescales and explored the relationship of synchrony to geographical distance. Synchrony was high at local scales of less than 1 km, with estimated Pearson correlations of approximately 0.6–0.8 between species' population growth rates across pairs of quadrats. Synchrony decayed by approximately 17–44% with each order of magnitude increase in distance but was still detectably positive at distances of 100 km and beyond. Dispersal cannot explain observed large-scale synchrony because typical seed dispersal distances (<100 m) are far too short to couple the dynamics of distant forests on decadal timescales. We attribute the observed synchrony in forest dynamics primarily to the effect of spatially synchronous environmental drivers (the Moran effect), in particular climate, although pests, pathogens and anthropogenic drivers may play a role for some species.

1. Introduction

Spatial synchrony in species' population dynamics has broad consequences for basic ecology and applied conservation [1]. Firstly, high spatial synchrony entails greater metapopulation extinction risk [2,3]. Secondly, high synchrony can lead to low stability of ecosystem function [4]. Thirdly, spatial synchrony poses challenges to theoretical community ecology. If synchrony were very high, this would validate the approach of many community models, which ignore spatial variation in population fluctuations (e.g. [5,6]). On the other hand, if synchrony were very low, this would motivate the application of mean-field approaches [7] to average independent fluctuations across space. But if synchrony is intermediate between these two extremes, more complex modelling approaches will be needed.

Spatial synchrony in population dynamics has been examined for insects [8–10], fish [11], crabs [12], birds [13,14], mammals [15,16] and viruses [17], and in many cases has been found to extend for hundreds or thousands of kilometres. There are two broad explanations for spatial synchrony [1,18]. The first is dispersal, which in theory can synchronize density-dependent population dynamics across space [1,18], even at scales substantially larger than the mean dispersal distance [19]. The second, referred to as the 'Moran effect' [15], is the dependence of population dynamics on spatially synchronous environmental variables, such as rainfall [1,16,18]. Synchrony of one species' population (via either dispersal or the Moran effect) can also drive synchrony in other species' populations via predator–prey or host–pathogen interactions [20]. Current empirical evidence for a range of species, from insects [21] to birds [22] to mammals [16,23], points to a dominant role of the Moran effect in driving spatial synchrony.

Comparatively little is known about the spatial synchrony in tree population dynamics. For mast-seeding species, synchrony of seed production occurs over large distances and has been attributed mainly to the Moran effect [24–26], but how this translates to synchrony of overall population dynamics, or to the majority of tree species that are not mast-seeders, is unknown. In the temperate zone, synchrony in the fossil pollen record has been observed at scales of *ca* 100 km, indicating the presence of some synchronizing mechanism—either dispersal or the Moran effect—over geological timescales [27]. But such fossil data are of limited use for quantifying the magnitude of synchrony over ecological timescales. Although there is clear evidence of synchrony in individual tree diameter growth rates (based on tree rings) on annual timescales across distances of up to 1000 km [28], it is unknown whether synchrony in diameter growth translates to synchrony in population growth (our focus here). The only study we are aware of that specifically measured synchrony in tree population growth rates used data from three large forest plots in central Panama over 3–5 years and found Pearson correlations in population growth rates of $r = 0.45–0.58$ over distances of 18–33 km [29].

Because of the tendency for tree species' populations to fluctuate strongly [30,31] and because trees are foundational species in ecosystems across the planet, it is essential to fill the knowledge gap about their spatial synchrony. On local scales, the statistical signature of tree population fluctuations is consistent with temporal variation in environmental conditions being their main driver [30,31]. In the permanent 50 ha ForestGEO plot on Barro Colorado Island (BCI) in Panama, the magnitude of the change in abundance of common tree species (species with more than 1000 individuals) was on average 28% over the period 1982–2010, which is more than ten times greater than one would expect under pure demographic stochasticity [30]. One particularly large abundance change (a 50% decline in the former canopy dominant *Poulsenia armata* over a decade) at BCI has been attributed to drought [30], and others have been attributed to insect outbreaks [32]. Similarly large fluctuations in tree abundance have been observed at other ForestGEO plots around the world, and have been attributed to hurricanes and typhoons, fires, elephants, and other environmental perturbations [6,30].

Our lack of knowledge about spatial synchrony of tree populations can be attributed to methodological challenges. Spatial synchrony for a single species can be assessed using standard statistical methods if sufficiently long time series are available [33], but most available time series of tree population dynamics are short relative to their estimated temporal autocorrelation period, which is roughly a decade [6,31]. A further difficulty in tropical forests is that most tree species are rare and population dynamics of rare species at scales of even several hectares are driven largely by demographic stochasticity, i.e. random fluctuations in population size arising from the discreteness of individuals [30]. Here, we apply novel statistical approaches to overcome these inherent methodological difficulties and estimate synchrony in tree population dynamics over five orders of magnitude of geographical distance. Our approach circumvents methodological difficulties by eschewing a per-species synchrony estimate and instead calculating an average synchrony estimate for each pair of observation units with at least one shared species. We leverage data from permanent forest plots on three spatial scales: the local scale, focusing on within-plot dynamics for two plots in the ForestGEO network; the regional scale, focusing on synchrony between 47 plots in the Marena network in central Panama; and the global scale, focusing on synchrony among 22 plots in the ForestGEO network.

2. Methods

(a) Data sources

We used data from permanent forest plots on three different spatial scales: local, regional and global. For the local scale, we used the two longest-established 50 ha plots in the ForestGEO network: the BCI plot in Panama, and the Pasoh plot in Malaysia. We used seven censuses of the BCI plot (from 1982 to 2010) and five censuses of the Pasoh plot (from 1987 to 2006). Each ForestGEO plot is censused at intervals of *ca* 5 years following a standard protocol, according to which all individual freestanding woody plants with diameter-at-breast-height (DBH; measured 1.3 m from the ground) ≥1 cm are identified and measured [34]. Individuals are tagged, which allows survival to be assessed across censuses. In our analyses, we used only main stems for trees with multiple stems.

For the regional scale, we used plots from the Marena network in central Panama [35]. We used only the 47 plots (out of a total of 65) that had been censused at least twice, to allow calculations of abundance fluctuations over time. All but two of these plots are 1 ha in size; one plot is 4 ha (Cocoli) and one is 5.96 ha (Sherman). The distances between pairs of the Marena plots used range from 0.3 km to over 200 km (electronic supplementary material, figure S1). These plots are censused using a similar protocol to the ForestGEO plots, except that in most of the 1 ha plots, a DBH threshold of 1 cm is used only in a 0.16 ha (40 m× 40 m) subplot, with a larger 10 cm threshold being used outside this.

For the global scale, we used 22 plots from the ForestGEO network (figure 1*a*; electronic supplementary material, appendix S1) that follow the standard ForestGEO measurement protocol described above for BCI and Pasoh. The selected plots had at least two censuses and areas of at least 12 ha. Inter-plot distances ranged from 138 km to nearly 20 000 km.

When describing methods that apply at all three scales we use the general term 'observation units' to refer to quadrats within plots in the local-scale analyses (BCI and Pasoh) and to entire plots in the regional analyses (Marena plots) and global-scale analyses (22 ForestGEO plots). Prior to assessing synchrony, we established which species were shared across observation units at each spatial scale (electronic supplementary material, appendix S2).

We estimated synchrony separately for each pair of observation units at each of the three focal scales. We ran one analysis for trees with ≥10 cm DBH and another for trees with ≥1 cm DBH. Repeating all of our analyses at two different DBH thresholds brought two advantages. Firstly, it allowed us to use more of the data: for the 1 cm threshold, we were able to include more trees overall, whereas for the 10 cm threshold, we were able to use the full spatial extent of the regional-scale plots (see methodological details below). Secondly, the analysis at each threshold reveals potentially distinct information about factors driving synchrony in population dynamics, in particular recruitment: synchrony of population dynamics for trees above 1 cm DBH will be strongly influenced by recent recruitment events, whereas that of trees above 10 cm DBH will be more reflective of recruitment events over several decades.

We use the term 'spatial grain' to refer to the size of the observation units (e.g. 1 ha plots) and 'spatial scale' to refer to the scale over which the observation units are spread (e.g. the regional scale). Ideally, analyses would be conducted at the largest spatial grains possible, to minimize the influences of demographic stochasticity and immigration (see §2c). But in practice, our choices of spatial grain were constrained by the data.

For the local-scale analyses, we subdivided the plot (i.e. BCI or Pasoh) in each analysis to create quadrats, which were the observation units. At the 10 cm DBH threshold, we ran the main analyses at a large spatial grain of 6.25 ha, to minimize the effects of immigration. We then repeated the analyses at a small spatial grain of 1 ha to facilitate comparison with the regional analysis for the same DBH threshold. At the 1 cm DBH threshold, we used three spatial grains: 6.25, 1 and 0.16 ha. The 0.16 ha grain here again facilitates comparison with the regional analysis at the same DBH threshold. Because the two plots in the local-scale analyses had dimensions 1000 × 500 m, when using the 0.16 ha grain we took the 0.16 ha quadrats from only a 1000 × 480 m sub-area of the plot in order to ensure that all quadrats were square.

For the regional-scale analyses we treated each plot as a separate observation unit and so the grain was 1 ha at the 10 cm DBH threshold and 0.16 ha at the 1 cm DBH threshold. For the two regional plots larger than 1 ha, we used data from a subplot of 1 ha (for the 10 cm DBH threshold) or 0.16 ha (for the 1 cm DBH threshold), which standardizes the grain across observation units at the expense of discarding some information. Only 34 regional plots could be used in the 1 cm DBH threshold analysis (0.16 ha grain), because in several Marena plots, the smaller stems were not censused or had been censused only once.

For the global-scale analyses, we treated each entire ForestGEO plot as a separate observation unit. A limitation of this is that the resulting observation units have different spatial grains, i.e. the ForestGEO plots have different areas. But the effects

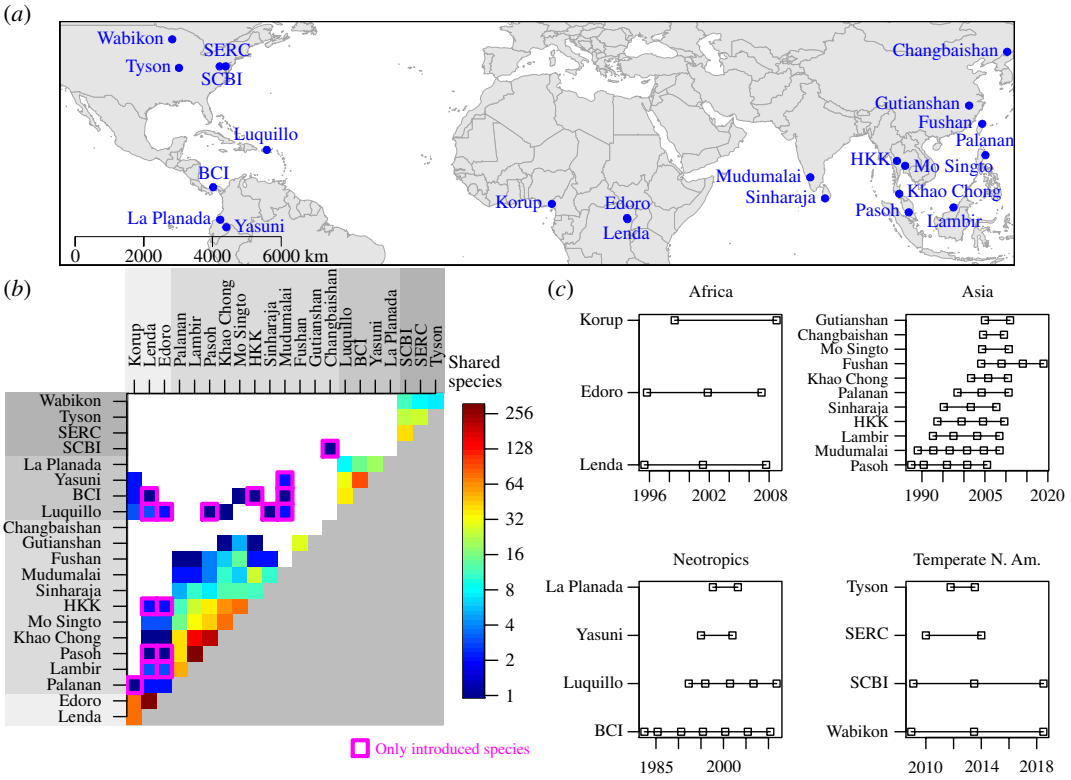

Figure 1. (*a*) Map of ForestGEO plots used in our global-scale analyses. (*b*) Within regions, most plots share some species, but between regions, few species are shared (levels of grey shading behind axis labels indicate region groupings, which are, from lightest to darkest: Africa, Asia, Neotropics, temperate North America). Almost all of the shared species between regions were introduced in at least one region (purple boxes indicate pairs of plots where all shared species fell into this category). (*c*) The census intervals overlapped to some extent for all pairs of plots with shared native species.

of this on the results should be minimal, because the minimum plot area was large (12 ha) and so the effects of demographic stochasticity and immigration should be small. Detailed acknowledgements for each plot are provided in electronic supplementary material, appendix S1.

(b) Synchrony metric

In this subsection, we define a general synchrony metric, which is independent of the details of the model we use in the next subsection to estimate it. Let synchrony ς_i be the Pearson correlation between the population growth rates of species i at two observation units, A and B, over time. A positive population growth rate means a species is increasing in abundance; a negative population growth rate means a species is decreasing in abundance. A synchrony value of $\varsigma_i = 1$ would imply that the species' population growth rate at observation unit A is exactly proportional to and of the same sign as the rate at observation unit B; a synchrony value of $\varsigma_i = -1$ would imply that the species' population growth rate at observation unit A is exactly proportional but of opposite sign to that at observation unit B; and a synchrony value of $\varsigma_i = 0$ would imply that the species' population growth rate at observation unit A is uncorrelated with that at observation unit B.

Although ideally one would estimate a separate value of ς_i for each of the species shared between two observation units, in our application to forest trees this is infeasible because of data limitations, mainly associated with the shortness of the census time series relative to the temporal autocorrelation period of forest tree population dynamics [31]. For this reason, for each pair of observation units, we estimate the average synchrony ς for all shared species, which is an average of the species-specific synchrony values ς_i. We emphasize that we are still conceptualizing each species as having its own distinct synchrony value ς_i, but we are unable to estimate these species-specific values, which we acknowledge as an inevitable methodological limitation given the data. The conceptual relationship between species-specific synchrony and the average synchrony metric is explained further in electronic supplementary material, appendix S2 (see in particular electronic supplementary material, figures S2 and S3).

(c) Estimating synchrony

In this subsection, we describe the model we used to estimate the average synchrony ς for each pair of observation units. In our datasets, the main source of uncertainty when estimating synchrony is demographic stochasticity, which can cause realized population growth rates at an observation unit to vary substantially from the expected rates, eroding the signal of synchrony. Demographic stochasticity has stronger effects in smaller populations. This is important in our analyses because many forest tree species are rare. Henceforth, when we use the term 'population growth rate' without qualification, we are referring to expected population growth rates uncontaminated by demographic stochasticity, i.e. the rates that we would measure in the limit of very large sample sizes (large numbers of trees).

We accounted for the influence of demographic stochasticity by using a mechanistic model that allows us to effectively assign lower weight to rare species when estimating average synchrony. In the model, abundance dynamics are driven by a combination of demographic stochasticity and fluctuations in population growth rates over time that are assumed to be driven by temporal environmental stochasticity [30]. Specifically, the abundance N_{x,i,t_2} of species i at observation unit x at time t_2 is modelled as a random variable that is the sum of a binomial survival term and a Poisson recruitment term:

$$N_{x,i,t_2} \sim \mathrm{Bi}(N_{x,i,t_1}, \theta_{x,i,t_1,t_2}) + \mathrm{Pois}(N_{x,i,t_1}(\lambda_{x,i,t_1,t_2} - \theta_{x,i,t_1,t_2})), \tag{2.1}$$

where N_{x,i,t_1} is the species' initial abundance, and λ_{x,i,t_1,t_2} and θ_{x,i,t_1,t_2} are the population growth rate and survival rate of species i at observation unit x from t_1 to t_2. The model assumes that there is a negative correlation between survival and recruitment rates across species, as represented by the presence of the parameter θ_{x,i,t_1,t_2} in both the survival and the recruitment terms in equation (2.1) (the quantity $1-\theta_{x,i,t_1,t_2}$ reflects the inherent turnover rate of species i and would typically be high for understorey shrubs and low for canopy trees). The model also assumes that survival and recruitment can be treated additively (i.e. recruitment occurs before mortality, and new recruits do not die or contribute to reproduction in the time interval considered). This assumption will have minimal effect on our results provided that the time interval $\Delta t = t_2 - t_1$ is substantially shorter than the generation time of trees. To enable comparability across fits to data with different time intervals Δt, we convert the λ and θ parameters for each species to an instantaneous population growth rate $\rho_{x,i,t_1,t_2} = (1/\Delta t)\log\lambda_{x,i,t_1,t_2}$ and an instantaneous mortality rate $\mu_{x,i} = -(1/\Delta t)\log\theta_{x,i,t_1,t_2}$. The model is hierarchical because these instantaneous rate parameters are drawn randomly and independently from hyperdistributions. We assume that the random variation in μ, and hence θ, represents life-history variation in turnover rates across species and is thus independent of time, and that the random variation in ρ, and hence λ, represents temporal environmental stochasticity. These assumptions and the structure of equation (2.1) imply that the effects of temporal environmental stochasticity are manifested in recruitment but not in mortality. This restriction is necessary because of data limitations imposed by the shortness of the census time series: allowing temporal environmental stochasticity in both recruitment and mortality would lead to parameter identifiability issues, as explained in [30] (see also [36]). Thus, synchrony in ρ between two observation units in the model is driven by synchrony in recruitment. Following [30], we used a lognormal distribution for μ and an asymmetric Laplace distribution for ρ.

Our model differs from that of [30] only in one crucial aspect: we replace the asymmetric Laplace distribution with its bivariate counterpart for the set of species that are shared across the two observation units, thus allowing the population growth rates of these species to be coupled across the observation units. We implemented the bivariate asymmetric Laplace distribution as a transformation of a bivariate standard normal distribution with correlation parameter ζ via a copula—a multivariate cumulative distribution function that links the underlying one-dimensional marginal cumulative distribution functions [37]. Copulas are used to model multivariate statistical phenomena in various fields, including quantitative finance. Once the parameters of the bivariate asymmetric Laplace distribution have been estimated for a given pair of observation units, our synchrony metric ς can be estimated by drawing a large number of pairs of population growth rates from the parameterized distribution and calculating the correlation between them. We emphasize that the copula parameter ζ is not the parameter of actual interest but rather a parameter that facilitates construction and fitting of a bivariate model, from which one can ultimately estimate synchrony ς, the parameter of actual interest (over most of model parameter space, ζ is numerically very close to ς though not exactly equal to it). In the limit of very large abundances (large $N_{x,i}$), i.e. when demographic stochasticity becomes negligible, our method simply produces an estimate of ς that is equal to the unweighted mean of the species-specific synchrony values (ς_i). In the presence of demographic stochasticity, the method effectively gives a weighted mean with more weight on common species, whose population growth rates are estimated with more certainty. In electronic supplementary material, appendix S2, we describe the mathematical structure of our model in more detail.

One limitation of our model is that it assumes that all recruits arise from reproduction within a given observation unit, i.e. it assumes that immigration constitutes a negligible fraction of the propagule rain. This assumption will be better for larger observation units: immigrants constitute only approximately 10% of the propagule rain in a 50 ha observation unit or 20% in a 6.25 ha observation unit, but approximately 70% in a 0.16 ha observation unit [38]. To the extent that adult tree density outside a focal observation unit differs from that within the observation unit, immigration will act as a source of noise that erodes the signal of synchrony in population growth rates between two observation units. Thus, our synchrony estimates will tend to underestimate true synchrony in population growth rates, particularly at smaller spatial grains, which we acknowledge as a limitation of our methods.

Before fitting the model to data, for each pair of observation units, we took the longest time period covered by both observation units' census histories. For the local analyses, this was simply the entire census history (28 years at BCI and 19 years at Pasoh), because all quadrats in a plot are included in each census. For the regional and global analyses, this often involved trimming the census history of one or both plots. For example, in the global analysis, we had census data for Pasoh spanning 1987–2006 and for Lambir spanning 1993–2008, so the comparison period for Pasoh versus Lambir was 1993–2006. In most cases, interpolation of abundances at one or both observation units was necessary to match the start and end dates (t_1 and t_2) of a comparison period. We did this by taking the two censuses with census dates closest to the comparison start or end date, and using these to interpolate the abundances at the start or end date, assuming constant mortality and recruitment rates for each species between the two censuses (electronic supplementary material, appendix S2). We performed a similar interpolation procedure for numbers of survivors of each species from the start to the end date (electronic supplementary material, appendix S2), as these values were also needed as model inputs to allow separate estimation of the survival and recruitment terms in equation (2.1).

We fitted the model to the data for each pair of observation units with at least one shared species by maximizing the likelihood of the hierarchical model using a Gibbs sampler with a Metropolis update rule [39–41] (see electronic supplementary

material, appendix S2). Given observed abundances N_{A,i,t_1}, N_{A,i,t_2}, N_{B,i,t_1} and N_{B,i,t_2} for each species i present at two observation units (A and B) and at each of two timepoints t_1 and t_2, as well as the number of survivors of each species at each observation unit from timepoint t_1 to t_2, the fitting process estimates the five parameter values of the two hyperdistributions (two for the lognormal and three for the asymmetric Laplace) at each observation unit, the copula parameter ζ linking the asymmetric Laplace distributions of population growth rates for shared species across the two observation units, as well as the instantaneous population growth rate for each species present at the two observation units ($\rho_{A,i}$ and $\rho_{B,i}$) and the corresponding mortality rates ($\mu_{A,i}$ and $\mu_{B,i}$). Thus, the total number of estimated parameters is $2(2+3)+1+2(S_A+S_B)$, where S_A and S_B are the number of species present at observation units A and B, respectively. The estimate of the copula parameter ζ is mainly informed by the shared species across two observation units, although the non-shared species have an indirect influence because they inform the estimates of model parameters other than ζ, which are algebraically linked to ζ via the likelihood function (electronic supplementary material, appendix S2).

We provide details on the fitting procedure with the Gibbs sampler in electronic supplementary material, appendix S2. A workflow diagram of our method for estimating synchrony is shown in electronic supplementary material, figure S4. We validated our method by fitting the model to simulated data with known synchrony (electronic supplementary material, figure S5). We also tested the robustness of the synchrony metric ς to census intervals of different lengths using our local-scale data (BCI and Pasoh).

(d) Assessing the relationship between synchrony and distance

After estimating synchrony values at a given scale (local, regional or global), we fitted power-law decay functions to quantify how synchrony between forest communities depends on geographical distance. Prior to fitting the power laws, we transformed synchrony values from the interval $(-1, 1)$ to the interval $(-\infty, \infty)$ using $z = \tan(\varsigma\pi/2)$. This transformation serves two purposes: it ensures that synchrony values from the fitted models cannot be outside the range $(-1, 1)$ and it improves model fits because near $\varsigma = -1$ and $\varsigma = 1$ the estimate of z is close to unbiased, whereas the estimate of ς from our maximum likelihood procedure is slightly biased towards 0 (see §3). We estimated confidence intervals on the decay functions by bootstrapping over observation units [42]. In addition to fitting power laws, we also fitted smoothing splines to the data to assess potential idiosyncratic trends in synchrony with geographical distance.

3. Results

(a) Local analyses

Estimated synchrony among populations of tree species within each of our two ForestGEO plots used for the local analyses (BCI and Pasoh) was positive and generally high. At the largest spatial grain (6.25 ha), across all pairs of observation units, the estimated value of the synchrony metric ς was on average 0.80 and 0.68 for the 1 and 10 cm DBH thresholds, respectively, at BCI (inter-census interval = 28 years), and 0.72 and 0.59 at Pasoh (inter-census interval = 19 years) (figure 2). Estimates of synchrony were robust to the length of the inter-census interval used (electronic supplementary material, figure S6). At the smaller spatial grains (1 and 0.16 ha), estimated synchrony at both plots was somewhat lower (electronic supplementary material, figures S7 and S8), which we attribute to the effects of higher *per capita* immigration at these grains (see §2).

Distance decay in synchrony was broadly similar across the two plots and spatial grains. For trees with ≥10 cm DBH, at BCI, the estimated decay was 27% per order of magnitude of distance at the 6.25 ha spatial grain, and 29% at the 1 ha spatial grain; at Pasoh the corresponding estimates were 27 and 17%. For trees with ≥1 cm DBH, the decay estimates at BCI were 17, 29 and 30% for the 6.25, 1 and 0.16 ha spatial grains, and at Pasoh they were 38, 44 and 36%.

(b) Regional analysis

In the regional analysis (the 1 ha Marena plots in central Panama), over 90% of plot pairs had shared species and could be included in the analysis: of these, the mean number of shared species at the 10 cm DBH threshold was 30.4, and at the 1 cm DBH threshold was 16.3 (recall that the census area was smaller at the lower DBH threshold). The most frequently occurring species were *Virola sebifera* at the 10 cm DBH threshold (39 out of 47 plots) and *Sorocea affinis* at the 1 cm DBH threshold (33 out of 34 plots).

Synchrony at the regional scale (Marena plots) was high at the shortest distances (<0.5 km) but substantially lower at the longest distances (>200 km) (figure 3). Although uncertainty was large for any given pair of plots, the overall trend in synchrony across all pairs of plots was robust. The four pairs of plots separated by a distance of less than 0.5 km had estimated synchrony values ς of on average 0.43 (1 cm DBH) and 0.52 (10 cm DBH) (figure 3), consistent with the magnitude of synchrony estimated in the local-scale analyses (figure 2). The estimated rate of decay in synchrony over one order of magnitude of distance was 26% for trees with ≥10 cm DBH, and 44% for trees with ≥ 1 cm DBH, comparable to the decay observed at the local scale.

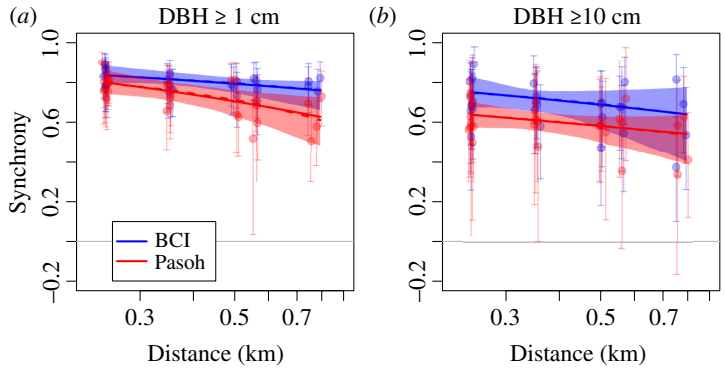

Figure 2. In our local-scale analyses (using BCI and Pasoh forest plots only), spatial synchrony in forest tree dynamics was high and declined with distance (0.1–1 km). Results for trees with (*a*) DBH ≥1 cm and (*b*) DBH ≥10 cm, in quadrats of size 6.25 ha (250 × 250 m) within the BCI forest plot (blue) and the Pasoh forest plot (red). Each point indicates the estimated average synchrony metric (Pearson correlation in population growth rates) for all species shared between two quadrats (vertical axis) and the geographical distance between the quadrats (horizontal axis). For trees with DBH ≥1 cm (*a*), the average number of species shared between two quadrats (observation units) was 212 and 618 for BCI and Pasoh, respectively; for DBH ≥10 cm (*b*), the corresponding numbers were 139 and 344. Whiskers indicate the 95% credible intervals on each synchrony estimate. Solid curves show power-law fits to the overall relationship between synchrony and distance, with shaded regions showing 95% confidence intervals. Dashed curves (almost perfectly coinciding with the solid curves on these graphs) show smoothing splines.

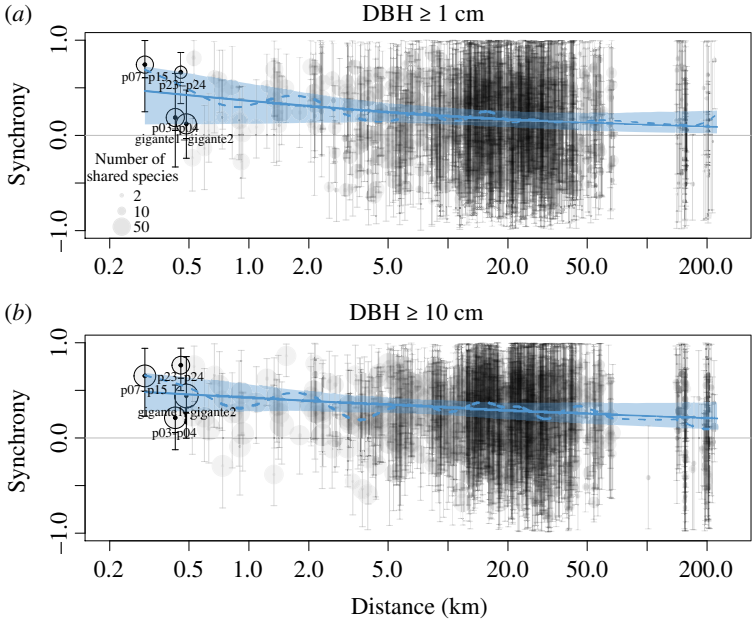

Figure 3. In our regional-scale analyses, spatial synchrony in forest tree dynamics was moderate and declined with distance (0.3–200 km). Each point is the estimated synchrony between two forest plots in the Marena network in central Panama, with whiskers showing 95% credible intervals. The synchrony estimates are computed as in figure 2. The size of each point is proportional to the number of species shared between the two corresponding plots (see graphical legend in (*a*)). The curves are power-law fits, with details as described in caption for figure 2. The four nearest pairs of plots are labelled (see map in electronic supplementary material, figure S1). (*a*,*b*) Results for trees with DBH ≥1 cm and DBH ≥10 cm, respectively.

(c) Global analysis

At the global scale, our 22 plots had an average area of 29.8 ha. Eleven of the plots were in Asia, four were in temperate North America, four were in the Neotropics, and three were in Africa (figure 1*a*). The time intervals between censuses used in the analyses ranged from 2 years at Tyson Research Center (TRC) to 28 years at BCI. Our ability to measure synchrony in the global analysis was dependent on overlap in the species composition between ForestGEO plots, most of which are hundreds or thousands of kilometres apart, and also on overlap in the timing of the censuses to create a congruent census interval. Of the more than 4600 species in our dataset, a total of 1132 were present at more than one plot, and 330 of these were present at more than two plots (see electronic supplementary material, appendix S3 for more details). Unsurprisingly, most observed species overlap was among plots within each of the four major geographical regions, with minimal overlap for different geographical regions (figure 1*b*). Of the few species shared between plots in different geographical regions, most were introduced in at least one of the regions (figure 1*b*). We did not exclude introduced species from our analyses, but the relatively small number of introduced species and their low abundances meant their impact on measured synchrony, and thus the overall results, was minimal. Most plot pairs with shared species exhibited some overlap in overall census interval (figure 1*c*).

Estimated synchrony varied widely across plot pairs, and in some cases across DBH thresholds for a given plot pair, but was slightly positive on average (figure 4). Uncertainty in synchrony estimates was in most cases high because of low statistical

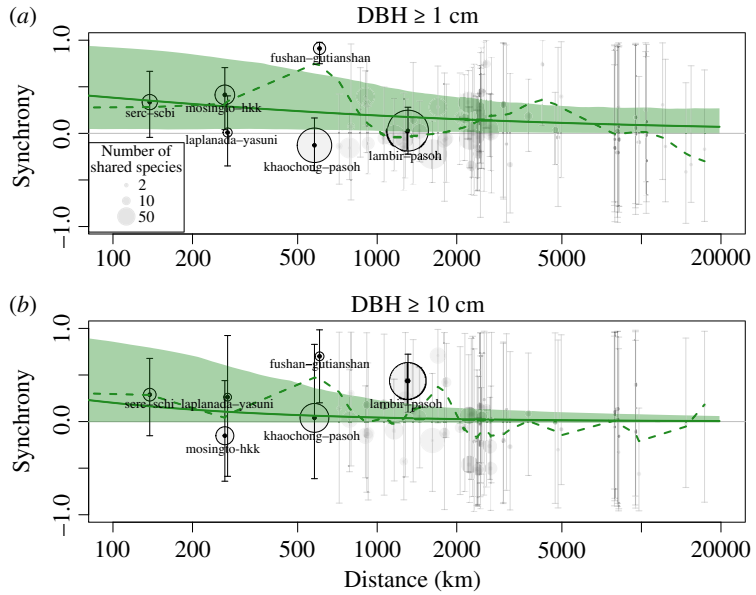

Figure 4. In our global-scale analyses, spatial synchrony in forest tree dynamics was positive on average but low and declined with distance (100–20 000 km). Details are as for figure 3. The five nearest pairs of plots are labelled, along with Lambir–Pasoh (the pair of plots with the second-highest number of shared species, after Edoro–Lenda; see figure 1*b*). (*a*, *b*) Results for trees with DBH ≥1 cm and DBH ≥10 cm, respectively.

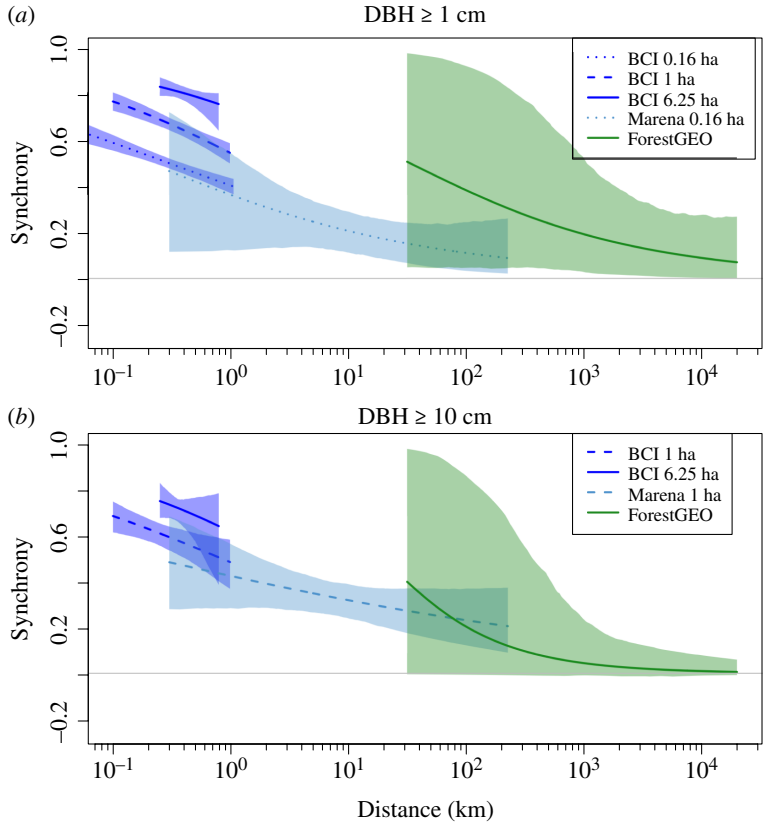

Figure 5. Spatial synchrony in forest tree dynamics declined consistently from local to global scales. Shown together are the fitted power laws (see graphical legends) from figure 2 for the local BCI scale in Panama (dark blue curves), figure 3 for the Marena regional scale in central Panama (light blue curves), and figure 4 for the global ForestGEO scale (green curves; all plots), along with fits for smaller spatial grains at BCI (dashed and dotted dark blue curves; see electronic supplementary material, figures S7 and S8) to facilitate direct comparison with the Marena data. Synchrony is lower at smaller spatial grains, which we attribute to the decorrelating effects of immigration over yearly to decadal timescales (see text). (*a*, *b*) Results for trees with DBH ≥1 cm and DBH ≥10 cm, respectively.

power (attributable to the low number of shared species between most pairs of plots). The estimated rates of decay in synchrony over one order of magnitude of distance were 68% for trees of ≥10 cm DBH and 34% for trees of ≥1 cm DBH, but uncertainty in these values was again high.

4. Discussion

We have shown for the first time pervasive large-scale synchrony in tree species' population growth rates, from local to global scales (figure 5). Broadly, there are two classes of mechanism that can drive synchrony in a species' population dynamics across space: the environment and dispersal [1,18]. The former is referred to as the Moran effect, after Moran [15], who showed that in the special case that the logarithm of species' abundance follows linear dynamics with environmental noise, the expected synchrony in population dynamics is exactly equal to the synchrony in the environmental variable. Nonlinearities in population dynamics refine this picture but do not fundamentally change the expectation of a close correspondence between synchrony in population growth and environmental variables [23]. In our tree population data, we estimated synchrony in population growth rates to be of the order of $\varsigma = 0.5$ (Pearson correlation) at scales of hundreds of kilometres and to be detectably positive even at scales of thousands of kilometres (figure 5). Synchrony in climate variables extends up to thousands of kilometres, with 'teleconnections' at the largest scales associated with phenomena such as the El Niño-Southern Oscillation [43]. The magnitude of synchrony in rainfall and synchrony in temperature varies globally and is not strictly distance-dependent, but it is consistently greater than $r = 0.5$ (Pearson correlation) at scales of 100 km [22] and is thus sufficient to explain our observed tree population synchrony. Spatial synchrony in other climate variables, such as winds from hurricanes [44] and typhoons [45], may also play a role, but our sample size (22 plots at the global scale) is too low to pinpoint the exact climate drivers with statistical confidence. Future studies with data from more plots may facilitate this.

The alternative explanation of dispersal being the primary driver of population dynamics [18] is not plausible for our forest communities. Dispersal-induced synchrony can occur because exchange of individuals between observation units tends to equalize population density and, assuming density-dependent dynamics, this tends to equalize population growth rates [18]. These effects cannot account for the high synchrony observed in our data because tree population density varied broadly across observation units at all scales. For example, within the 50 ha BCI plot, the average coefficient of variation in a tree species' density over quadrats was greater than 0.6 at all three spatial grains. A further piece of evidence against the dispersal hypothesis is that we even observed statistically detectable synchrony between pairs of plots that are biogeographically isolated from each other. For example, the Fushan and Gutianshan plots are separated by a total distance of 600 km, including the 180 km Taiwan Strait, and yet estimated synchrony between the two plots was high (figure 4).

Perhaps counterintuitively, in our data, the effect of dispersal is actually to erode the signal of synchrony, particularly for small observation units. The reason is that our model assumes immigrant propagules are a small fraction of total propagules at an observation unit and can thus be ignored when calculating the population growth rate, an assumption which for trees likely only holds at spatial grains above 1 ha. This effect is clearly visible in our analyses at different spatial grains at the local scale (electronic supplementary material, figures S7 and S8; figure 5). Because of these immigration effects, our estimates of synchrony represent lower bounds on true synchrony in population growth rates, especially in our regional-scale analysis where our maximum spatial grain was constrained by the small plot sizes: 1 ha for trees with DBH ≥10 cm and 0.16 ha for trees with DBH ≥1 cm. Based on comparisons of measured synchrony across spatial grains in our local-scale analyses (figures 2 and 5; electronic supplementary material, figures S7 and S8), we can infer that true synchrony at the regional scale (i.e. the synchrony that would be observed at a larger spatial grain where the effects of immigration become negligible) is substantially higher than the measured values. For example, we infer true synchrony of $\varsigma \approx 0.4$ for trees with DBH ≥10 cm at a distance of 20 km (from figure 5*b*).

The drivers of synchrony may be more complicated for tree species impacted by spatially synchronized intertrophic interactions, in particular pest and pathogen outbreaks. For example, Dutch elm disease has driven widespread declines of the tree species *Ulmus americana* and *Ulmus rubra* in North America over nearly a century [46]. This disease has been implicated in these two tree species' declines at our SCBI plot [47], and the same two species have also declined at our other North American plots. However, even for insect outbreaks, the weight of evidence points mainly towards the Moran effect, rather than dispersal, as the main driver of synchrony [48–50]. Thus, even in cases where the proximate driver of spatial synchrony in tree population dynamics is a pest or pathogen, the ultimate driver may still be the Moran effect. A final set of additional potential drivers of synchrony in tree population dynamics are anthropogenic influences. Although these could be broadly construed as a subclass of intertrophic interactions, they warrant separate consideration. A case in point is the species *Aquilaria malaccensis*, which has declined consistently over time at all three of our Asian ForestGEO plots where it is present and it is known to be illegally harvested for agarwood [51] in at least one of these plots. Air pollution is another spatially correlated human impact that can impact trees' vital rates [52]. The relative importance of these anthropogenic drivers, versus the Moran effect, for synchrony in tree population dynamics is a topic for further study.

Our estimates of spatial synchrony in forest dynamics can inform metapopulation models that seek to estimate species' extinction risk. Populations whose dynamics are highly synchronized over their geographical range are at greater risk of extinction because the constituent subpopulations tend to decline together [2,3]. The median global range size of tree species found in Panama is 6.9×10^5 km^2 [53], corresponding to a linear range extent of the order of 1000 km, a distance at which we estimated average synchrony in population dynamics to be positive but with very broad credible intervals (figure 4), suggesting that a species with median range size may be buffered from extinction by spatially desynchronized population fluctuations. Nevertheless, 16.2% of Panama tree species have a range size of less than 20 000 km^2, corresponding to a linear range extent closer to 100 km, a scale at which synchrony is detectable with more statistical certainty (figure 3), suggesting greater vulnerability to extinction of this subgroup.

Our novel statistical method for assessing synchrony of population dynamics across observation units, using an average metric for multiple species, is broadly applicable to datasets involving large numbers of species with time series of abundances that are short relative to the temporal autocorrelation period of population dynamics. In such cases, standard time-series

analysis methods for single populations [33] are not applicable because there are too few independent data points. A strength of our method is that the fitting procedure implicitly gives each species an appropriate weight that is inversely related to the uncertainty in its population growth rate (electronic supplementary material, appendix S2); for rare species, this uncertainty is greater because of demographic stochasticity, and the weights are thus lower (electronic supplementary material, appendix S2). An alternative and simpler method would be just to discard rare species below some abundance threshold and to look at synchrony in the population growth rates of the common species [29], obviating the use of mechanistic models and likelihood maximization. But this approach discards valuable information contained in the dynamics of the rare species shared between observation units: rare species typically compose the majority of shared species in diverse tropical tree communities, particularly in small forest plots (≤1 ha). Our methods are also robust to the time interval between censuses (electronic supplementary material, figure S6): synchrony between a pair of observation units fluctuates over time (as has also been observed for mammal populations [54]), but these fluctuations are small relative to the average value.

There are several caveats to our method. Firstly, our method assumes that environmental stochasticity affects recruitment but not mortality. This assumption is necessary owing to data limitations associated with short time series but appears to be justified [30]. As noted, our method also does not account for the effects of immigration, but the direction of the bias arising from immigration is known (it is towards lower synchrony; see §2), and the bias can in principle be minimized by using larger observation units. Another limitation of our method is that, by design, it gives an average synchrony value across all shared species between two observation units (ς). This masks potential interspecific variation in synchrony, which may be of biological interest but could only be explored with longer time series (enabling species-specific estimates of synchrony, ς_i).

Our results also have implications for species coexistence theory [55–57]. Traditional explanations for high tropical tree diversity have focused on equilibrium models of isolated forest plots. Such explanations include Janzen–Connell effects and resource niches [55,58]. But it is increasingly recognized that tree populations are incredibly dynamic and are interconnected with conspecific populations throughout the landscape [6,30,31,59]. Extending the perspective of coexistence theory to regional and continental scales requires knowledge of how local tree populations in different places fluctuate relative to one another over a range of spatial extents—estimates of which we have provided here. We noted above that range-restricted tree species will be especially vulnerable to extinction owing to synchronized population dynamics. Our synchrony estimates place constraints on the minimum strength of coexistence mechanisms required for range-restricted species to coexist at the landscape scale with widespread species whose fluctuations are buffered by metapopulation effects.

Ethics. This work did not require ethical approval from a human subject or animal welfare committee.

Data accessibility. Code and data for running analyses have been deposited in Zenodo [60].

Supplementary material is available online [61].

Declaration of AI use. We have not used AI-assisted technologies in creating this article.

Authors' contributions. R.A.C.: conceptualization, data curation, funding acquisition, methodology, writing—original draft, writing—review and editing; T.F.: data curation, methodology, writing—review and editing; K.J.A.-T.: data curation, writing—review and editing; N.A.B.: data curation; W.Y.B.: data curation; S.B.: data curation; C.-H.C.-Y.: data curation; Y.-Y.C.: data curation; G.B.C.: data curation; R.C.: writing—review and editing; H.S.D.: data curation; S.J.D.: writing—review and editing; S.E.: data curation; C.E.N.E.: data curation; E.S.F.: data curation; I.A.U.N.G.: data curation; C.V.S.G.: data curation; Z.H.: data curation; R.W.H.: data curation; D.K.: data curation; T.L.Y.: data curation; J.-R.M.: data curation; S.M.M.: data curation, writing—review and editing; X.M.: data curation; M.B.M.: data curation; J.A.M.: data curation, writing—review and editing; A.N.: data curation; Á.J.P.: data curation; S.P.: data curation; N.P.: data curation; H.R.: data curation; L.J.V.R.: data curation; R.S.: data curation; I.-F.S.: data curation; H.S.S.: data curation; D.W.T.: data curation; J.T.: data curation, writing—review and editing; M.U.: data curation; R.V.: data curation; X.W.: data curation; A.T.W.: data curation; J.K.Z.: data curation.

All authors gave final approval for publication and agreed to be held accountable for the work performed herein.

Conflict of interest declaration. We declare we have no competing interests.

Funding. R.A.C. and T.F. acknowledge support from Singapore's Ministry of Education (grant number WBS A-8001046-00-00).

Acknowledgements. We thank David Nott for helpful discussions. A full list of acknowledgements for each ForestGEO plot is provided in electronic supplementary material, appendix S1.

References

1. Lande R, Engen S, Sæther BE. 1999 Spatial scale of population synchrony: environmental correlation versus dispersal and density regulation. *Am. Nat.* **154**, 271–281. (doi:10.1086/303240)
2. Harrison S, Quinn JF. 1989 Correlated environments and the persistence of metapopulations. *Oikos* **56**, 293–297. (doi:10.2307/3565613)
3. Heino M, Kaitala V, Ranta E, Lindström J. 1997 Synchronous dynamics and rates of extinction in spatially structured populations. *Proc. R. Soc. Lond. B* **264**, 481–486. (doi:10.1098/rspb.1997.0069)
4. Walter JA *et al*. 2021 The spatial synchrony of species richness and its relationship to ecosystem stability. *Ecology* **102**, e03486. (doi:10.1002/ecy.3486)
5. Kalyuzhny M, Seri E, Chocron R, Flather CH, Kadmon R, Shnerb NM. 2014 Niche versus neutrality: a dynamical analysis. *Am. Nat.* **184**, 439–446. (doi:10.1086/677930)
6. Fung T *et al*. 2020 Temporal population variability in local forest communities has mixed effects on tree species richness across a latitudinal gradient. *Ecol. Lett.* **23**, 160–171. (doi:10.1111/ele.13412)
7. Fung T, Pande J, Shnerb NM, O'Dwyer JP, Chisholm RA. 2024 Processes governing species richness in communities exposed to temporal environmental stochasticity: a review and synthesis of modelling approaches. *Math. Biosci.* **369**, 109131. (doi:10.1016/j.mbs.2023.109131)
8. Pollard E. 1991 Synchrony of population fluctuations: the dominant influence of widespread factors on local butterfly populations. *Oikos* **60**, 7–10. (doi:10.2307/3544985)
9. Hanski I, Woiwod IP. 1993 Spatial synchrony in the dynamics of moth and aphid populations. *J. Anim. Ecol.* **62**, 656–668. (doi:10.2307/5386)
10. Sutcliffe OL, Thomas CD, Moss D. 1996 Spatial synchrony and asynchrony in butterfly population dynamics. *J. Anim. Ecol.* **65**, 85–95. (doi:10.2307/5702)

11. Myers RA, Mertz G, Bridson J. 1997 Spatial scales of interannual recruitment variations of marine, anadromous, and freshwater fish. *Can. J. Fish. Aquat. Sci*. **54**, 1400–1407. (doi:10.1139/f97-045)
12. Botsford LW, Moloney CL, Hastings A, Largier JL, Powell TM, Higgins K, Quinn JF. 1994 The influence of spatially and temporally varying oceanographic conditions on meroplanktonic metapopulations. *Deep Sea Res. II Top. Stud. Oceanogr.* **41**, 107–145. (doi:10.1016/0967-0645(94)90064-7)
13. Lindström J, Ranta E, Lindén H. 1996 Large-scale synchrony in the dynamics of capercaillie, black grouse and hazel grouse populations in Finland. *Oikos* **76**, 221–227. (doi:10.2307/3546193)
14. Koenig WD. 1998 Spatial autocorrelation in California land birds. *Conserv. Biol*. **12**, 612–620. (doi:10.1111/j.1523-1739.1998.97034.x)
15. Moran PAP. 1953 The statistical analysis of the Canadian lynx cycle. *Aust. J. Zool.* **1**, 291–298. (doi:10.1071/ZO9530291)
16. Grenfell BT, Wilson K, Finkenstädt BF, Coulson TN, Murray S, Albon SD, Pemberton JM, Clutton-Brock TH, Crawley MJ. 1998 Noise and determinism in synchronized sheep dynamics. *Nature* **394**, 674–677. (doi:10.1038/29291)
17. Bolker BM, Grenfell BT. 1996 Impact of vaccination on the spatial correlation and persistence of measles dynamics. *Proc. Natl Acad. Sci. USA* **93**, 12648–12653. (doi:10.1073/pnas.93.22.12648)
18. Liebhold A, Koenig WD, Bjørnstad ON. 2004 Spatial synchrony in population dynamics. *Annu. Rev. Ecol. Evol. Syst*. **35**, 467–490. (doi:10.1146/annurev.ecolsys.34.011802.132516)
19. Satake A, Iwasa Y. 2002 Spatially limited pollen exchange and a long-range synchronization of trees. *Ecology* **83**, 993–1005. (doi:10.1890/0012-9658(2002)083[0993:SLPEAA]2.0.CO;2)
20. Vasseur DA, Fox JW. 2009 Phase-locking and environmental fluctuations generate synchrony in a predator–prey community. *Nature* **460**, 1007–1010. (doi:10.1038/nature08208)
21. Haynes KJ, Bjørnstad ON, Allstadt AJ, Liebhold AM. 2013 Geographical variation in the spatial synchrony of a forest-defoliating insect: isolation of environmental and spatial drivers. *Proc. R. Soc. B* **280**, 20122373. (doi:10.1098/rspb.2012.2373)
22. Koenig WD. 2002 Global patterns of environmental synchrony and the Moran effect. *Ecography* **25**, 283–288. (doi:10.1034/j.1600-0587.2002.250304.x)
23. Blasius B, Stone L. 2000 Nonlinearity and the Moran effect. *Nature* **206**, 846–847. (doi:10.1038/35022646)
24. Koenig WD, Mumme RL, Carmen WJ, Stanback MT. 1994 Acorn production by oaks in central coastal California: variation within and among years. *Ecology* **75**, 99–109. (doi:10.2307/1939386)
25. Koenig WD, Knops JMH. 2000 Patterns of annual seed production by Northern Hemisphere trees: a global perspective. *Am. Nat*. **155**, 59–69. (doi:10.1086/303302)
26. Ashton PS, Givnish TJ, Appanah S. 1988 Staggered flowering in the Dipterocarpaceae: new insights into floral induction and the evolution of mast fruiting in the aseasonal tropics. *Am. Nat*. **132**, 44–66. (doi:10.1086/284837)
27. Ostling AM. 2012 Large-scale spatial synchrony and the stability of forest biodiversity revisited. *J. Plant Ecol*. **5**, 52–63. (doi:10.1093/jpe/rtr035)
28. Shestakova TA *et al*. 2016 Forests synchronize their growth in contrasting Eurasian regions in response to climate warming. *Proc. Natl Acad. Sci. USA* **113**, 662–667. (doi:10.1073/pnas.1514717113)
29. Condit R, Aguilar S, Hernandez A, Perez R, Lao S, Angehr G, Hubbell SP, Foster RB. 2004 Tropical forest dynamics across a rainfall gradient and the impact of an El Niño dry season. *J. Trop. Ecol*. **20**, 51–72. (doi:10.1017/S0266467403001081)
30. Chisholm RA *et al*. 2014 Temporal variability of forest communities: empirical estimates of population change in 4000 tree species. *Ecol. Lett*. **17**, 855–865. (doi:10.1111/ele.12296)
31. Kalyuzhny M, Kadmon R, Shnerb NM. 2015 A neutral theory with environmental stochasticity explains static and dynamic properties of ecological communities. *Ecol. Lett*. **18**, 572–580. (doi:10.1111/ele.12439)
32. Fung T, O'Dwyer JP, Rahman KA, Fletcher CD, Chisholm RA. 2016 Reproducing static and dynamic biodiversity patterns in tropical forests: the critical role of environmental variance. *Ecology* **97**, 1207–1217. (doi:10.1890/15-0984.1)
33. Gouhier TC, Guichard F. 2014 Synchrony: quantifying variability in space and time. *Methods Ecol. Evol*. **5**, 524–533. (doi:10.1111/2041-210X.12188)
34. Condit R. 1998 *Tropical forest census plots: methods and results from Barro Colorado Island, Panama and a comparison with other plots*. Berlin, Germany: Springer-Verlag.
35. Condit R, Pérez R, Aguilar S, Lao S. 2019 Census data from 65 tree plots in Panama, 1994-2015. Dryad Digital Repository. (doi:10.15146/mdpr-pm59)
36. Melbourne BA, Hastings A. 2008 Extinction risk depends strongly on factors contributing to stochasticity. *Nature* **454**, 100–103. (doi:10.1038/nature06922)
37. Nelsen RB. 1999 *An introduction to copulas*. New York, NY: Springer.
38. Chisholm RA, Lichstein JW. 2009 Linking dispersal, immigration and scale in the neutral theory of biodiversity. *Ecol. Lett*. **12**, 1385–1393. (doi:10.1111/j.1461-0248.2009.01389.x)
39. Rüger N, Huth A, Hubbell SP, Condit R. 2009 Response of recruitment to light availability across a tropical lowland rain forest community. *J. Ecol*. **97**, 1360–1368. (doi:10.1111/j.1365-2745.2009.01552.x)
40. Gelman A, Carlin JB, Stern HS, Rubin DB. 1995 *Bayesian data analysis*. Boca Raton, FL: Chapman and Hall/CRC.
41. Condit R *et al*. 2006 The importance of demographic niches to tree diversity. *Science* **313**, 98–101. (doi:10.1126/science.1124712)
42. Bjørnstad ON, Ims RA, Lambin X. 1999 Spatial population dynamics: analyzing patterns and processes of population synchrony. *Trends Ecol. Evol.* **14**, 427–432. (doi:10.1016/S0169-5347(99)01677-8)
43. Feldstein SB, Franzke CLE. 2017 Atmospheric teleconnection patterns. In *Nonlinear and stochastic climate dynamics* (eds CLE Franzke, TJ O'Kane), pp. 54–104. Cambridge, UK: Cambridge University Press.
44. Canham CD, Thompson J, Zimmerman JK, Uriarte M. 2010 Variation in susceptibility to hurricane damage as a function of storm intensity in Puerto Rican tree species. *Biotropica* **42**, 87–94. (doi:10.1111/j.1744-7429.2009.00545.x)
45. Yap SL, Davies SJ, Condit R. 2016 Dynamic response of a Philippine dipterocarp forest to typhoon disturbance. *J. Veg. Sci*. **27**, 133–143. (doi:10.1111/jvs.12358)
46. Brasier CM. 2000 Intercontinental spread and continuing evolution of the Dutch elm disease pathogens. In *The elms: breeding, conservation, and disease management* (ed. CP Dunn), pp. 61–72. Boston, MA: Springer US.
47. Anderson-Teixeira KJ *et al*. 2021 Long-term impacts of invasive insects and pathogens on composition, biomass, and diversity of forests in Virginia's Blue Ridge mountains. *Ecosystems* **24**, 89–105. (doi:10.1007/s10021-020-00503-w)
48. Zhang Q, Alfaro RI. 2003 Spatial synchrony of the two-year cycle budworm outbreaks in central British Columbia, Canada. *Oikos* **102**, 146–154. (doi:10.1034/j.1600-0706.2003.12169.x)
49. Peltonen M, Liebhold AM, Bjørnstad ON, Williams DW. 2002 Spatial synchrony in forest insect outbreaks: roles of regional stochasticity and dispersal. *Ecology* **83**, 3120–3129. (doi:10.1890/0012-9658(2002)083[3120:SSIFIO]2.0.CO;2)
50. Johnson DM, Liebhold AM, Bjørnstad ON, Mcmanus ML. 2005 Circumpolar variation in periodicity and synchrony among gypsy moth populations. *J. Anim. Ecol*. **74**, 882–892. (doi:10.1111/j.1365-2656.2005.00980.x)

51. Zhang L, Brockelman WY, Allen MA. 2008 Matrix analysis to evaluate sustainability: the tropical tree *Aquilaria crassna*, a heavily poached source of agarwood. *Biol. Conserv*. **141**, 1676–1686. (doi:10.1016/j.biocon.2008.04.015)
52. Dietze MC, Moorcroft PR. 2011 Tree mortality in the eastern and central United States: patterns and drivers. *Glob. Chang. Biol*. **17**, 3312–3326. (doi:10.1111/j.1365-2486.2011.02477.x)
53. Condit R, Aguilar S, Pérez R. 2020 Trees of Panama: a complete checklist with every geographic range. *For. Ecosyst*. **7**, 13. (doi:10.1186/s40663-020-00246-z)
54. Ranta E, Kaitala V, Lundberg P. 1998 Population variability in space and time: the dynamics of synchronous population fluctuations. *Oikos* **83**, 376–382. (doi:10.2307/3546852)
55. Broekman MJE, Muller-Landau HC, Visser MD, Jongejans E, Wright SJ, de Kroon H. 2019 Signs of stabilisation and stable coexistence. *Ecol. Lett*. **22**, 1957–1975. (doi:10.1111/ele.13349)
56. Chesson P. 2000 Mechanisms of maintenance of species diversity. *Annu. Rev. Ecol. Syst*. **31**, 343–366. (doi:10.1146/annurev.ecolsys.31.1.343)
57. Barabás G, D'Andrea R, Stump SM. 2018 Chesson's coexistence theory. *Ecol. Monogr.* **88**, 277–303. (doi:10.1002/ecm.1302)
58. Hülsmann L, Chisholm RA, Hartig F. 2021 Is variation in conspecific negative density dependence driving tree diversity patterns at large scales? *Trends Ecol. Evol.* **36**, 151–163. (doi:10.1016/j.tree.2020.10.003)
59. Condit R, Chisholm RA, Hubbell SP. 2012 Thirty years of forest census at Barro Colorado and the importance of immigration in maintaining diversity. *PLoS One* **7**, e49826. (doi:10.1371/journal.pone.0049826)
60. Chisholm RA. 2024 Data from: Assessing the spatial scale of synchrony in forest tree population dynamics. Zenodo. (doi:10.5281/zenodo.14064127)
61. Chisholm R, Fung T, Anderson-Teixeira K, Bunyavejchewin S, Chang-Yang CH, Chen YY. 2024 Supplementary material from: Assessing the spatial scale of synchrony in forest tree population dynamics. Figshare. (doi:10.6084/m9.figshare.c.7508869)